

Nd³⁺ ion shift under domain inversion by electron beam writing in LiNbO₃

P. Molina,^{a)} D. Sarkar, M. O. Ramírez, J. García Solé, and L. E. Bausá
Departamento de Física de Materiales, Universidad Autónoma de Madrid, 28049-Madrid, Spain

B. J. García
Departamento de Física Aplicada, Universidad Autónoma de Madrid, 28049-Madrid, Spain

J. E. Muñoz Santiuste
Departamento de Física, Escuela Politécnica Superior, Universidad Carlos III de Madrid, Leganes, 28911 Madrid, Spain

(Received 16 February 2007; accepted 1 March 2007; published online 4 April 2007)

Ferroelectric domain inversion has been obtained in Nd³⁺ doped lithium niobate by means of direct electron beam writing. The local effects of the polarization inversion on the optical transitions of Nd³⁺ ions have been studied by low temperature high resolution site selective spectroscopy. Inverted regions present different axial crystal field acting over Nd³⁺ ions compared with noninverted (original) regions. The results can be interpreted in terms of slight shifts of Nd³⁺ ions along the ferroelectric *c* axis within the Li⁺ octahedrons, as a result of the lattice rearrangement after the domain inversion processes. © 2007 American Institute of Physics. [DOI: 10.1063/1.2719036]

Direct electron beam writing has been recently shown as a very promising technique to fabricate domain reversed structures in LiNbO₃ because of its versatility and high resolution, which can lead to high quality photonic devices.^{1,2} For instance, nonlinear photonic crystals, in which the sign of the second order nonlinear susceptibility χ^2 is modulated, can be envisaged.³ On the other hand Nd³⁺ is without any doubt the paradigm among the lasing ions. It is then of particular relevance to investigate the fabrication of domain reversed structures in Nd³⁺ doped LiNbO₃ crystals, so that future multifunctional solid state lasers based on LiNbO₃:Nd³⁺ nonlinear photonic crystals could be realized. As for any other domain inversion technique the use of direct electron beam writing could produce structural changes affecting the optical transitions of Nd³⁺ ions, and so the laser properties of a multifrequency emitter laser device based on this system.

In this work, we have applied the direct electron beam writing technique for domain inversion in Nd³⁺ doped LiNbO₃ crystals. Then, the effect of domain inversion on the luminescence of Nd³⁺ in LiNbO₃ has been systematically investigated by means of high spectral resolution site selective spectroscopy with spatial resolution in the micrometer range. Site selective spectroscopy is a very powerful technique for determining very weak structural changes around the emitting Nd³⁺ ions and for revealing the presence of different nonequivalent Nd³⁺ centers, i.e., Nd³⁺ ions subjected to slightly different local structural environments.⁴

A congruent ([Li]/[Nb]=0.945) LiNbO₃ single domain crystal doped with a Nd³⁺ ion concentration of 0.1 wt % was grown by the Czochralski method in our laboratory. From this crystal a 500 μm thickness plate was cut and polished with its main faces oriented perpendicular to the ferroelectric *c* axis. Prior to the electron beam bombardment the *c*⁺ face of the sample was coated with a 100 nm thick film of Al, which acted as a ground electrode. Direct electron beam writing was carried using a Philips XL30 Schottky field

emission gun scanning electron microscope; the irradiation parameters were 25 keV incident electron energy on the *c*⁻ face, 200 pA irradiation current, and 40 mC/cm² equivalent dose. The irradiated patterns were large enough regions (of about 10 × 10 μm^2) in order to facilitate the spectroscopic experiments over individual domains.

Figure 1 shows the *y* face of the sample after chemical etching (in a 2:1 solution of HNO₃:HF at 60 °C for 20 min). A polarization domain-inverted region between two noninverted domains is clearly revealed. As can be seen, it is important to note how the irradiation process on the *c*⁻ face produces effective polarization inversion across the whole sample thickness. Previous works have demonstrated the good optical quality and homogeneity of these large sized domain-inverted regions, pointing out that under our conditions the electron bombardment does not substantially affect

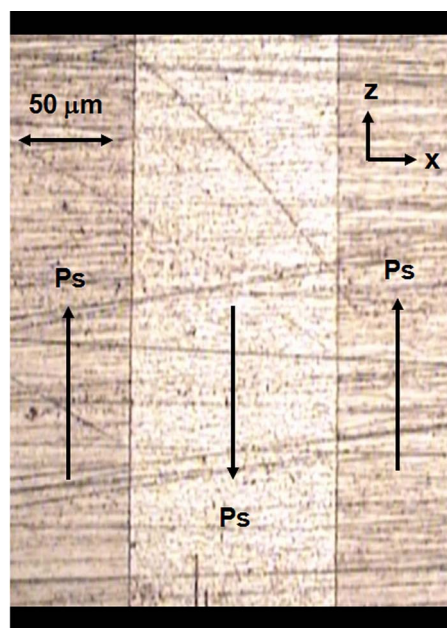


FIG. 1. (Color online) Lateral view, along the *y* face, of the domain inverted between two noninverted domains after chemical etching.

^{a)}Electronic mail: pablo.molina@uam.es

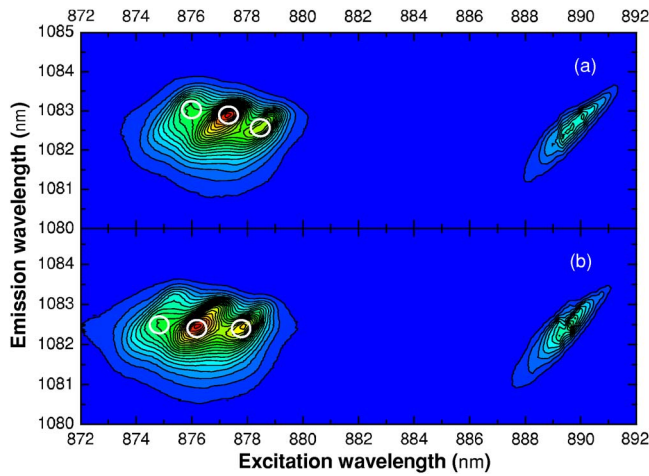


FIG. 2. (Color online) Compared contour plot of the total site spectrum of ${}^4I_{9/2} \rightarrow R_1, R_2$ excitations and $R_1 \rightarrow 1({}^4I_{11/2})$ emission of Nd^{3+} ions in LiNbO_3 : (a) inverted region and (b) original region.

the structural characteristics of the reversed structures.² In fact, it has been shown that neither the room temperature Raman nor the room temperature Nd^{3+} luminescence spectra were affected by the electron irradiation.

In this work, all the spectroscopy experiments were realized by excitation with the laser beam perpendicular to the poled c^- face. High resolution laser site selective spectroscopy (SSS) at low temperature (10 K) was used in order to investigate the effect of polarization inversion on the Nd^{3+} optically active centers as a result of electron irradiation. This includes the use of the so-called total site selective spectroscopy (TSSS). This technique, which has been applied to detect trivalent rare earth centers in LiNbO_3 , is a powerful tool that provides “spectroscopic maps” obtained from recorded three dimensional (excitation wavelength, emission wavelength, and intensity) spectra, from which different centers can be unequivocally detected.^{5–7}

In our experiments the beam of a tunable Ti:sapphire laser was focused by means of a $100\times$ microscope objective (with an estimated spot size of around $1\ \mu\text{m}$) into the different inverted and noninverted domain regions, so that it has been possible to compare the Nd^{3+} spectra coming from both types of ferroelectric domains. The emitted light was collected and directed onto a double grating spectrometer and detected with a charge-coupled device detector.

Previous details on the spectroscopic properties of Nd^{3+} in LiNbO_3 can be found elsewhere.^{4,8,9}

As a relevant example of the TSSS technique, Fig. 2 shows the contour plots obtained under excitation of both inverted (a) and original (b) regions in the excitation wavelength range from 872 to 892 nm (including ${}^4I_{9/2} \rightarrow R_1$ and ${}^4I_{9/2} \rightarrow R_2$ transitions) and monitoring specific $R_1 \rightarrow 1({}^4I_{11/2})$ emission transition (from 1080 to 1085 nm). An inspection of the TSSS spectroscopic map of Fig. 2(b) reveals the presence of three nonequivalent Nd^{3+} centers, which, for the sake of clarity, have been marked by the circles displayed in the $1 \rightarrow R_1$ excitation wavelength range.

According to previous TSSS data, these centers correspond to the so-called Nd-1, Nd-2, and Nd-3 centers which appear in congruent $\text{LiNbO}_3:\text{Nd}$ crystals.^{10,11} By combining Rutherford backscattering spectrometry/channeling and SSS techniques¹⁰ these three centers were related to Nd^{3+} ions located in Li^+ octahedrons but shifted from the regular Li^+

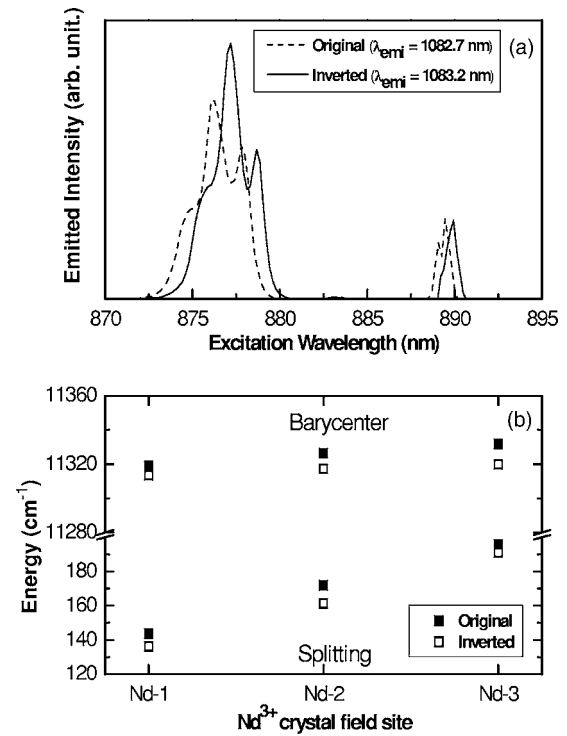


FIG. 3. Excitation spectra for the original and inverted domains. (b) Amount of splitting and barycenter of the ${}^4F_{3/2}$ state for the nonequivalent Nd^{3+} centers in the original and inverted domains.

lattice position towards the nearest oxygen plane⁹ by three different amounts along the ferroelectric c axis. The reason for these three different displacements within the Li^+ octahedron must be the different charge compensation mechanisms because of the excess of charge of Nd^{3+} ions relative to the Li^+ lattice ions. As has been suggested, these charge compensation mechanisms can occur at the cost of Li^+ vacancies.¹¹

As can be seen from Fig. 2(a) these three Nd centers are present in both the original and the inverted domain regions. However, the spectroscopic features of both regions are slightly different: in particular, the excitation-emission maxima of the spectra (circles) are slightly shifted.

To gain information on the changes observed in the Nd-1, Nd-2, and Nd-3 centers in the inverted domain regions, we focus our attention the relevant ${}^4F_{3/2}$ excited state. This state splits into two states only by deviations from the cubic symmetry. In the case of LiNbO_3 the amount of this splitting gives a measure of the trigonal (C_3) crystalline field around the Nd^{3+} ions in the different centers. On the other hand, the barycenter position of the ${}^4F_{3/2}$ state is useful in comparing Nd^{3+} centers related to different lattice sites, i.e., in different arrangements (position, distance, type, and number) of the ligand ions (near neighbors).

Figure 3(a) shows, for the sake of comparison, two ${}^4I_{9/2} \rightarrow R_1, R_2$ excitation spectra obtained when monitoring at the wavelengths corresponding to the maximum emission intensity from the original and inverted domains. The presence of the Nd centers is clearly appreciated in the triplet structure observed over the ${}^4I_{9/2} \rightarrow R_2$ excitation (absorption) component. The Nd-1, Nd-2, and Nd-3 centers, respectively, peak at 877.7, 876.2, and 874.9 nm in the original (nonirradiated) ferroelectric domain while these centers shift their peaks to longer wavelengths in the inverted domains, 878.6 nm (Nd-

1), 877.2 nm (Nd-2), and 875.8 nm (Nd-3). These spectra allow to obtain the splitting and barycenter for the ${}^4F_{3/2}$ state. Figure 3(b) shows the amount of splitting and the barycenter of the ${}^4F_{3/2}$ state for the Nd-1, Nd-2, and Nd-3 centers in the original and inverted domains. It can be seen that the trigonal splitting is different from one center to another. Indeed this fact is related to a different shift of the Nd^{3+} ions in each center relative to the Li^+ location (which is also off centered in the lithium octahedron). As can be appreciated, the trigonal splitting of the Nd^{3+} centers decreases in the inverted domain together with a slight modification in their barycenter positions. These results lead to an obvious indication: a rearrangement in the local environment of the Nd^{3+} ions (centers) takes place in the electron beam irradiated region.

At this point it is important to mention that rearrangements in the center structure of Er^{3+} ions in LiNbO_3 have been also reported in reversed domains obtained by application of an electric field.¹² In addition, these local structural changes could be at the base of the differences observed in the coercive fields for domain inversion in the forward and backward directions previously reported for undoped LiNbO_3 .¹³

Let us now discuss the possible local structure modifications leading to these optical lines for the Nd-1, Nd-2, and Nd-3 centers. It is important to remember that these centers are associated with three different shifts of the Nd^{3+} ions along the c axis with respect to the regular Li^+ position.^{4,10,11} The amount of trigonal splitting in the ${}^4F_{3/2}$ is governed by the B_0^2 crystal field parameter (the splitting in the ${}^4F_{3/2}$ can be easily estimated as $0.16B_0^2$ in Wybourne normalization assuming that this state is isolated), and so it may change from one Nd^{3+} center to another. In a simple overlap model based on the ligand point charge approximation this crystal field parameter is given by^{14,15}

$$B_0^2 = \rho \left(\frac{2}{1+\rho} \right)^3 \sum_j \frac{g_j}{\rho_j^3} \frac{1}{2} (3x_j^2 - 1) \langle r^2 \rangle, \quad (1)$$

where ρ is the overlap coefficient for the Nd–O bonding, $g_j=2$ is the number of electron ligand charges, ρ_j are the Nd^{3+} to O^{2-} distances in the Li^+ octahedron, $x_j = \cos \alpha_j$ gives the cosine directors of the ligand ions, and $\langle r^2 \rangle = 1.001 a_0^{-2}$ (a_0 being the Bohr radius) denotes the integral of the $4f$ Nd^{3+} radial function.¹⁶ Figure 4 shows the dependence of B_0^2 on the c axis position of the Nd^{3+} ion in the Li^+ octahedron. It can be seen how B_0^2 (and therefore the amount of ${}^4F_{3/2}$ splitting) increases with the shift with respect to the regular Li^+ position (0 Å in Fig. 4). As a possible interpretation, we propose that the Nd^{3+} ions in the inverted domains are less shifted (0.02 Å) away from the regular Li^+ positions than those in the original domains.

In order to account for these Nd^{3+} ion shifts by domain inversion we have to invoke the principle of ferroelectric domain inversion in lithium niobate. It has been proposed that this is consistent with the movement of Li^+ ions from their octahedrons to the free octahedrons, crossing the oxygen triangle (the one in the $x < 0$ direction in the inset of Fig. 4) under the influence of the electric field induced by the

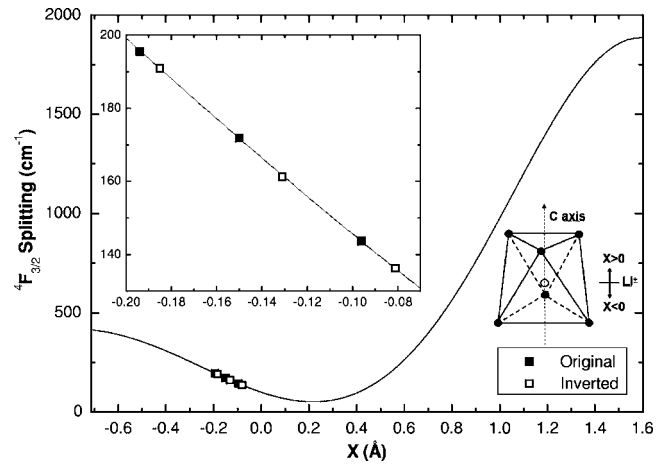


FIG. 4. Theoretical splitting of the ${}^4F_{3/2}$ state for the nonequivalent Nd^{3+} centers from Eq. (1). Experimental points for original and inverted regions are also shown.

electrons. Thus the initial Li–Nb–vacancy sequence is changed to a vacancy–Nb–Li sequence.¹⁷

In summary, ferroelectric domain inversion has been achieved in Nd^{3+} doped LiNbO_3 single domain crystals using the direct electron beam writing technique. This fact, together with the slight differences in the nonequivalent center structure for Nd^{3+} ions after domain inversion process compared with the original ones, allows to envisage the use of this versatile technique to fabricate active χ^2 nonlinear photonic laser crystals based on Nd^{3+} doped LiNbO_3 with the variety of designs required for different self-frequency conversion processes.

This work has been supported by the Spanish Ministry of Education and Science under Contract No. MAT2004-03347.

¹J. He, *J. Appl. Phys.* **93**, 9943 (2003).

²P. Molina, B. J. García, F. Agulló-Rueda, M. O. Ramírez, and L. E. Bausá, *Ferroelectrics* **343**, 334 (2006).

³V. Berger, *Phys. Rev. Lett.* **81**, 4136 (1998).

⁴J. García Solé, L. E. Bausá, D. Jaque, E. Montoya, H. Murrieta, and F. Jaque, *Spectrochim. Acta, Part A* **54**, 1571 (1998).

⁵D. M. Gill, J. C. Wright, and L. MaCaughan, *Appl. Phys. Lett.* **64**, 2483 (1994).

⁶J. García Solé, A. Lorenzo, T. Petit, G. Boulon, B. Roux, and H. Jaffrezic, *J. Phys. IV* **4**, 293 (1994).

⁷V. Dierolf, C. Sandmann, V. Gopalan, S. Kim, and K. Polgar, *Radiat. Eff. Defects Solids* **158**, 247 (2003).

⁸H. Loro, M. Voda, F. Jaque, J. García Solé, and J. E. Muñoz Santuste, *J. Appl. Phys.* **77**, 5929 (1995).

⁹A. Lorenzo, H. Jaffrezic, B. Roux, G. Boulon, and J. García Solé, *Appl. Phys. Lett.* **67**, 3735 (1995).

¹⁰J. García Solé, T. Petit, H. Jaffrezic, and G. Boulon, *Europhys. Lett.* **24**, 719 (1993).

¹¹A. Lorenzo, H. Loro, J. E. Muñoz Santuste, M. C. Terrile, G. Boulon, L. E. Bausá, and J. García Solé, *Opt. Mater. (Amsterdam, Neth.)* **8**, 55 (1997).

¹²V. Dierolf and M. Koerd, *Phys. Rev. B* **61**, 12 (2000).

¹³V. Gopalan, T. Mitchell, Y. Furukawa, and K. Kitamura, *Appl. Phys. Lett.* **72**, 1981 (1998).

¹⁴O. L. Malta, *Chem. Phys. Lett.* **88**, 3 (1982).

¹⁵M. Faucher and P. Caro, *J. Chem. Phys.* **63**, 446 (1975).

¹⁶A. J. Freeman and R. E. Watson, *Phys. Rev.* **127**, 2058 (1962).

¹⁷P. W. Haycock and P. D. Townsend, *Appl. Phys. Lett.* **48**, 698 (1986).